Prediction of tumor response and patient outcome after radioembolization of hepatocellular carcinoma using 90Y-PET-computed tomography dosimetry

Article *in* Nuclear Medicine Communications · March 2021

DOI: 10.1097/MNM.0000000000001395

CITATIONS
4

READS
36

8 authors, including:

d'abadie Philippe
Cliniques Universitaires Saint-Luc
26 PUBLICATIONS **56** CITATIONS
SEE PROFILE

Stephan Walrand
Cliniques Universitaires Saint-Luc
105 PUBLICATIONS **2,697** CITATIONS
SEE PROFILE

Michel Hesse
Université Catholique de Louvain - UCLouvain
64 PUBLICATIONS **979** CITATIONS
SEE PROFILE

Ivan Borbath
Cliniques Universitaires Saint-Luc
210 PUBLICATIONS **21,812** CITATIONS
SEE PROFILE

Original article

Nuclear Medicine Communications

Prediction of tumor response and patient outcome after radioembolization of hepatocellular carcinoma using ^{90}Y-PET-computed tomography dosimetry

Philippe d'Abadie[a], Stephan Walrand[a], Michel Hesse[a], Laurence Annet[b], Ivan Borbath[c], Marc Van den Eynde[c], Renaud Lhommel[a] and François Jamar[a]

Aim 90Y-radioembolization using glass or resin microspheres is increasingly used for the treatment of hepatocellular carcinoma (HCC). The aim of this retrospective study is to determine the prognostic relevance of dosimetric parameters defined with 90Y-PET-CT obtained immediately after radioembolization.

Methods Forty-five HCC patients, mostly with multiple lesions, were treated by radioembolization between 2011 and 2017. After treatment, all underwent a 90Y PET-CT with time of flight reconstruction (90Y-TOF-PET-CT). Tumor absorbed dose and cumulative tumor dose-volume histogram were calculated using a dose point Kernel convolution algorithm. The radiological tumor response was assessed using modified (m)-RECIST criteria. Progression-free-survival (PFS) and overall survival (OS) were analyzed using the Kaplan–Meier method and Cox regression analysis.

Results Twenty-six patients were treated with glass microspheres (73 lesions) and nineteen with resin microspheres (60 lesions). Thresholds of 118 and 61 Gy for glass and resin microspheres respectively correlate well with radiological response with a positive predictive value (PPV) of 98 and 80% and discriminate patient outcome with regard to PFS ($P = 0.03$ and 0.005) and OS ($P = 0.003$ and 0.007). Using dose volume histogram, a minimal absorbed dose of 40 Gy in 66% of the tumor volume (defined as D66) was highly predictive of radiological response (PPV = 94%), PFS ($P < 0.001$) and OS ($P = 0.008$), for either device.

Conclusion Dosimetric parameters obtained using 90Y-PET-CT are predictive of tumor response, PFS and OS. In clinical practice, a systematic dosimetric evaluation using 90Y PET should be implemented to help predicting patient outcomes. *Nucl Med Commun* 42: 747–754 Copyright © 2021 Wolters Kluwer Health, Inc. All rights reserved.

Nuclear Medicine Communications 2021, **42**:747–754

Keywords: patient outcome, hepatocellular carcinoma, ^{90}Y-PET-CT dosimetry, ^{90}Y radioembolization

Departments of [a]Nuclear Medicine, [b]Medical Imaging and [c]Gastroenterology and Oncology, Cliniques Universitaires Saint Luc, Université Catholique de Louvain, Brussels, Belgium

Correspondence to Philippe d'abadie, MD, Department of Nuclear Medicine, Cliniques Universitaires Saint Luc, 10 Avenue Hippocrate, 1200 Brussels, Belgium
Tel: +32 2 764 25 82; e-mail: philippe.dabadie@uclouvain.be

Received 23 September 2020 **Accepted** 24 January 2021

Introduction

Among loco-regional treatments in hepatocellular carcinoma (HCC), intra-arterial liver radioembolization is nowadays widely used. Patients classified as 'intermediate' or 'advanced' stages according to Barcelona clinic liver cancer (BCLC) criteria are suitable for liver radioembolization [1] and show good response rates [2]. Radioembolization is performed with intrahepatic injection of ^{90}Y-labeled microspheres or ^{166}Ho-labeled microspheres (Quiremspheres, Quirem Medical, Deventer, the Netherlands). Glass (TheraSphere, Boston Sientific, Boston, Massachusetts, USA) and resin (SIR-Spheres, Sirtex Medical Ltd., Sydney, Australia) microspheres can be used with similarly effective results [3]. Glass microspheres have a higher specific activity per sphere (2500 vs. 50 Bq) and a lesser number of particles is injected (1–8 million vs. 40–80 million) [4]. The manufacturers' recommended methods to calculate delivered activities are empirical for resin microspheres using the body surface area method and based on Medical Internal Radiation Dose for glass microspheres with an average target absorbed dose ranging from 80 to 150 Gy to the injected liver volume [5].

Early convincing tumor absorbed dose-response correlations were obtained from pretherapy ^{99m}Tc-MAA (^{99m}Tc-macroaggregated albumin) SPECT [6–8] and from posttherapy ^{90}Y bremsstrahlung SPECT [9,10]. During the last decade, following the introduction of the more accurate ^{90}Y-PET imaging modality [11,12] better correlations were found between microspheres deposition and absorbed doses [5]. The role of oxygenation was evidenced as a function of hemoglobin level [13,14]. Taking into account the dose distribution heterogeneity, as observed with the ^{90}Y-PET-based D_{70}, still improved the correlation [15,16]. In a pure dosimetry study, that is, censoring the patients from the follow up when performing an additional therapy, the ^{90}Y-TOF-PET (^{90}Y-PET with time of flight reconstruction) based equivalent uniform dose (EUD) reunified the glass and resin patient

 DOI: 10.1097/MNM.0000000000001395

survival probability per Gy [17]. This result further supports that the activity distribution heterogeneity observed in ^{90}Y TOF-PET postradioembolization mainly reflects the inhomogeneous spheres' distribution [18,19].

The aim of this study is to assess whether the ^{90}Y-TOF-PET/computed tomography (CT) based dose distribution can also predict the impact of the radioembolization step within a whole therapy course, that is, including the impact of the selection biases between glass and resin spheres radioembolization, and without censoring the patient of the follow up when performing a further conventional therapy, conventional meaning other than radioembolization.

Materials and methods

Patient characteristics and treatments

Data from 48 HCC patients referred to our institution for radioembolization between July 2011 and July 2017 (Table 1) were retrospectively analyzed after approval of the local ethics committee (2017/27JUI/334). Three patients were excluded because of the lack of ^{90}Y-PET-CT imaging (n = 2) or uncorrectable motion artifacts (n = 1).

Most had intermediate or advanced stage HCC (78%). Twenty-six patients were treated with glass and nineteen with resin microspheres. Fifty-nine liver radioembolization were performed according to standard guidelines [20]. Fourteen patients received two treatments within an interval ranging from 16 h to 16 months. Glass and resin microspheres were used in 34 and 25 treatments, respectively, with a median activity of 2.6 and 1.5 GBq at the injection time. Treatments with glass microspheres were performed 1 week after ^{90}Y calibration.

Table 1 Patients' characteristics

	Glass microspheres	Resin microspheres
Number of patients	26	19
Age (mean ± SD)	69 ± 12	71 ± 10
Men/women (%)	85/15	79/21
Cirrhosis (%)	77	63
Child A/B (%)	77/23	95/5
BCLC A/B/C (%)	23/39/38	21/68/11
Multifocal ≥5 (%)	31	47
Vascular invasion[a] (%)	38	10
Segmental portal vein (%)	19	0
Branch portal vein (%)	8	5
Main portal vein (partial; %)	11	5
Tumor size ≥5 cm[a] (%)	35	73
Bilobar tumor involvement (%)	42	47
Extra hepatic metastases[b] (%)	4 (lung and bone)	5 (lung)
Therapies before last radioembolization (%)	65	42
Radiofrequency–alcoholization (%)	8	16
Chemoembolization (%)	31	26
Radioembolization (%)	35	21
Tyrosine-kinase inhibitor (%)	0	11
Liver surgery (%)	4	5
Liver transplantation (%)	0	5
Therapies after last radioembolization (%)	38	37
External beam radiotherapy (%)	4	0
Chemoembolization (%)	8	16
Tyrosine-kinase inhibitor (%)	15	10
Liver surgery (%)	8	0
Liver transplantation (%)	0	5

BCLC, Barcelona clinic liver cancer.[a]Differences between groups are statistically significant ($P < 0.05$).[b]Detected after radioembolization and not related to death.

Vascular invasion was more frequent in patients treated with glass microspheres (38 vs. 10%; $P < 0.05$) and especially segmental portal thrombosis. Conversely, more patients (73 vs. 35%; $P < 0.05$) treated with resin microspheres had large tumors (size ≥5 cm).

Dose distribution assessment

Within 20 h following radioembolization, a 45-min-^{90}Y-PET-CT (Gemini TF 16, Philips Medical Systems, Cleveland, Ohio, USA) was acquired. ^{90}Y activity distribution was transformed into a 3D map of absorbed doses using a previously detailed method [12]. In short, reconstruction was performed with the 3D line of response-TOF blob-based Philips algorithm [two iterations, 33 subsets; reconstructed voxels of $(4\ \text{mm})^3$]. Voxel counts were converted in activity using the PET calibration factor and ^{90}Y positrons yield. Absorbed dose distributions of individual tumors were calculated by convolving the ^{90}Y activity distribution with a dose point Kernel algorithm, jointly with a spatial resolution recovery [12].

Lesions were delineated manually on pretherapy imaging using T1-weighted contrast-enhanced MRI (n = 50) or arterial contrast-enhanced CT-scan (n = 8, when there was a contraindication for MRI), using PMOD 3.7 (PMOD Technologies LLC, Zürich, Switzerland). Tumor volumes of interest (VOIs) were fused with the 3D map of tumor voxel doses on ^{90}Y-PET-CT images using a rigid transformation (PMOD 3.7). For all lesions, a cumulative dose-volume histogram (CDVH) was computed, and also the D_{66} defined as the minimum absorbed dose deposited in 66% of the tumor volume:

$$\mathrm{DVH}\left(D_{66}\right) = 66\% \tag{1}$$

A total of 73 and 60 lesions were analyzed after glass and resin microspheres radioembolization, respectively. For lesions treated in the previous 6 months, the absorbed dose was the cumulative dose of both treatments (n = 12).

Dosimetric parameters were analyzed retrospectively and did not influence patient management.

Tumor response evaluation

Only lesions with a transverse axis >10 mm were analyzed. Tumor response was assessed using recommended modified RECIST criteria (mRECIST) at the last time point available. Contrast-enhanced MRI or CT scan were obtained every 2 months until death or progression. Targeted lesions were assessed by a senior radiologist expert in liver tumors, blinded to tumor uptake and dosimetry data. At any time, response was defined as 30% decrease and progression as 20% increase of viable tumor (enhancing during the arterial phase) compared to baseline imaging. Moreover, a stable lesion 6 months after

therapy is categorized as a progressive lesion. The number of tumors per patient was 2.5 ± 1.8 and 2 ± 1.6 in the resin and glass microspheres groups (P = 0.06).

Patient outcome evaluation

Overall survival (OS) was defined as the time between radioembolization (first one if appropriate) and death from any cause. Progression-free survival (PFS) was defined as the time from radioembolization to objective progression in the liver or death.

Censoring was applied for patients still alive (OS analysis) or without objective progression at the last radiological time point realized (PFS analysis).

Only the largest lesion was analyzed for the OS and PSF in order to avoid excessive partial volume effect on the dose distribution assessment. All lesion sizes were above 20 mm except in one patient (15 mm). For univariate and multivariate analyses, all patients were combined using an effective tumor dose D_{eff}. For this purpose, the cut-off for resin microspheres absorbed dose was converted into an 'equivalent glass microspheres absorbed dose (Equ. Glass TD)' using a multiplication factor of 1.9, as explained in the discussion section. For univariate analysis, the following variables were evaluated: Equ. Glass TD, D_{66}, portal thrombosis, bilobar tumor involvement, total bilirubinemia ≥2 mg/dl, Child B score, tumor size ≥5 cm, stages BCLC B and C, anemia (Hb ≤ 10 g/dl), age ≥75 years. For multivariate analysis, variables with significant results in the univariate analysis were included.

Statistical analysis

Wilcoxon distribution-free comparison test or Student's t test were used to compare groups receiving different devices. Sensitivity (Se) was defined as the ability of the absorbed dose to predict radiological response, whereas specificity (Sp) was defined as the ability of the absorbed dose in predicting no radiological response. Absorbed dose thresholds for response were determined using receiver-operating characteristics (ROC) curves, analyzed with a freeware calculator from Johns Hopkins University [12]. Kaplan–Meier method with a log rank test was used for univariate analysis. Cox proportional hazard model was used for uni- and multivariate analyses. Analyses were conducted using Prism (version 7.0, GraphPad Software, La Jolla, California, USA) and IBM SPSS statistics software (version 25.0, Armonk, New York, USA). A P value <0.05 was considered significant.

Results

Tumor response

For glass microspheres, median absorbed doses were 194 Gy (70–1426 Gy) and 95 Gy (51–142 Gy) in responding and progressive lesions, respectively (P < 0.001). For resin microspheres, median absorbed doses were 102 Gy (55–568 Gy) and 46 Gy (0.4–314 Gy) in responding and progressive lesions, respectively (P < 0.001). In responding lesions, the absorbed doses were statistically higher with glass microspheres (P < 0.001) with a glass/resin tumor dose ratio of 1:9. ROC curves (Fig. 1a) demonstrated that the threshold of 118 Gy resulted in

Fig. 1

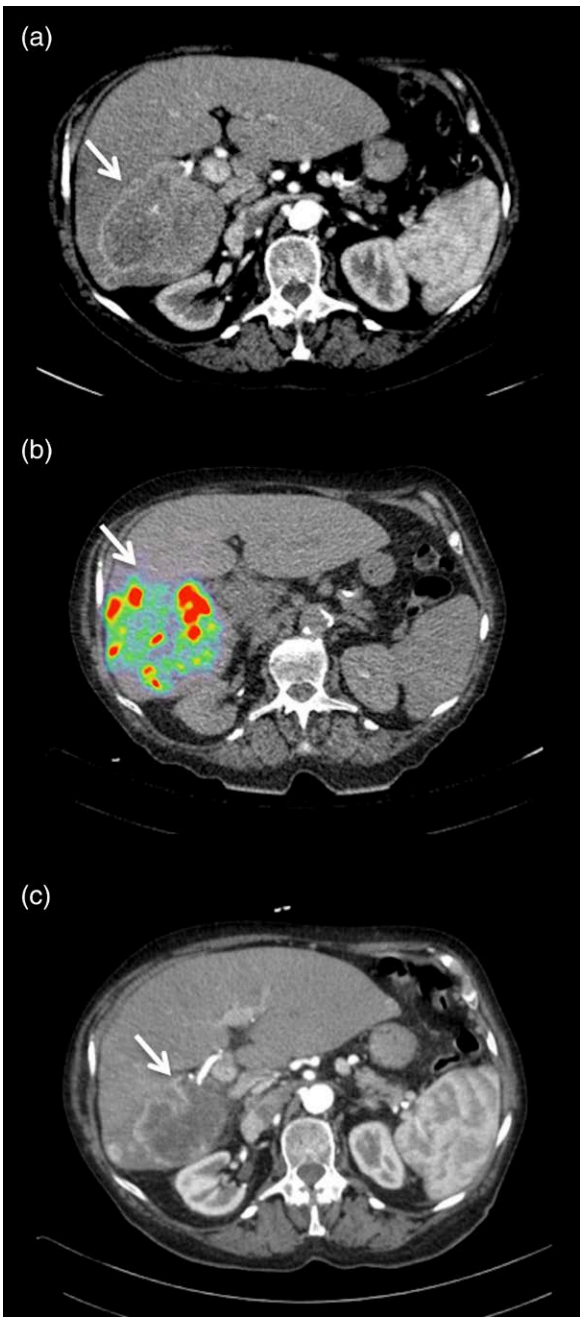

Example of large HCC lesion (white arrow) developed in the right liver on the arterial phase of the contrast-enhanced CT scan (a). ^{90}Y PET/CT (b) obtained just after glass microspheres therapy demonstrated an excellent tumor uptake (TD = 134 Gy, D_{66} = 81 Gy). Four months later, the CT scan confirmed an excellent radiological response with large tumor necrosis (c). CT, computed tomography; HCC, hepatocellular carcinoma.

Fig. 2

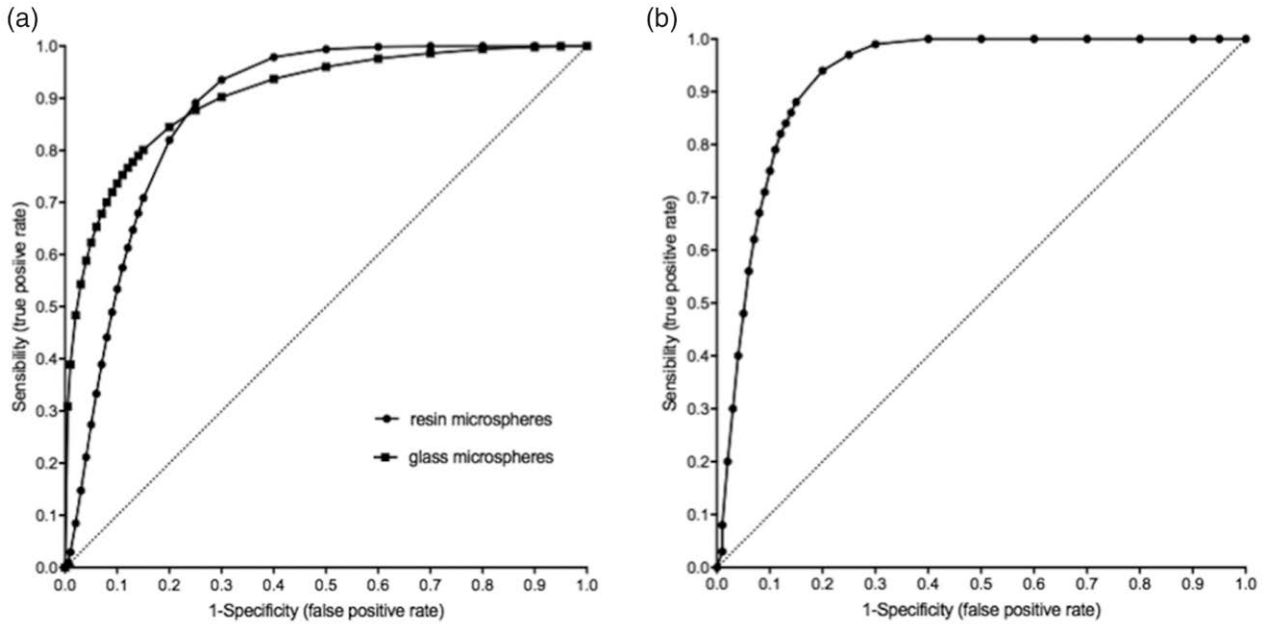

ROC curves for determination dose thresholds doses using TD (a) and CDVH with D66 (b). CDVH, cumulative dose-volume histogram; ROC, receiver-operating characteristics.

Fig. 3

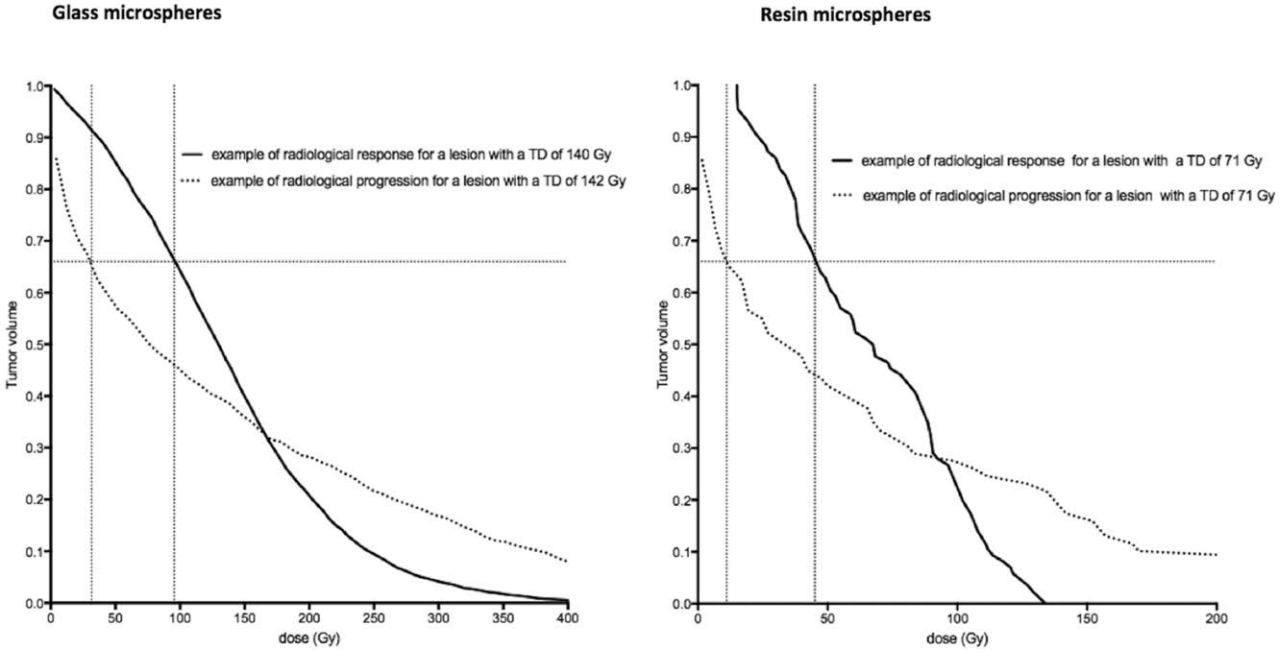

Examples of CDVH using glass (left) and resin microspheres (right). The CDVH are shown for examples of tumors with similar average doses but with different radiological responses. Using glass microspheres and two lesions with similar average doses (140–142 Gy), the lesion in response has a DVH characterized by $D_{66} = 96$ Gy and the lesion in progression has a DVH characterized by $D_{66} = 31$ Gy (grid lines). A similar behavior is found using resin microspheres for which the average dose is lower, that is, 71 Gy. CDVH, cumulative dose-volume histogram.

Table 2 Relation between tumor doses and prognosis for resin (threshold 61 Gy), glass microspheres (threshold 118 Gy) and using D_{66} (both types of spheres)

	Glass			Resin			D_{66} (resin and glass)		
	<118 Gy	≥118 Gy	All	<61 Gy	≥61 Gy	All	<40 Gy	≥40 Gy	All
Median OS (months)	5.6	14.6[a]	12.3	5.3	16[a]	13.4	6.5	16[a]	12.4
Median PFS (months)	1.8	5.5[b]	3	1.6	4.6[a]	2.9	1.8	5.4[c]	2.9

OS, overall survival; PFS, progression-free survival.[a]$P < 0.01$.[b]$P < 0.05$.[c]$P < 0.001$.

Fig. 4

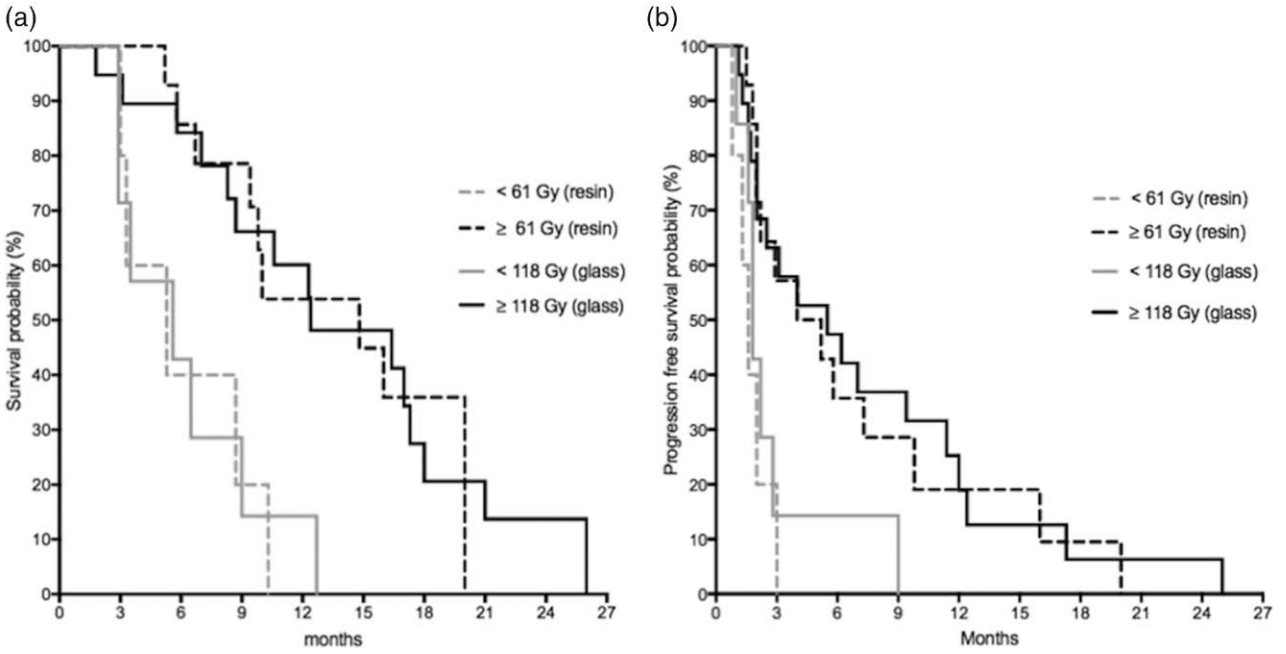

OS (a) and PFS (b) analyses with the Kaplan–Meier method for glass microspheres with a threshold dose of 118 Gy and resin microspheres with a threshold dose of 61 Gy.

the best prediction of tumor response using glass microspheres [Se = 93%; Sp = 75%; positive predictive value (PPV) = 98%, NPV = 50%, AUC = 0.91 ± 0.08]; the threshold was 61 Gy using resin microspheres (Se = 87%, Sp = 64%, PPV = 98%, NPV = 80%, AUC = 0.88 ± 0.07). Figure 2 shows an example of HCC imaging before and after treatment in comparison to ^{90}Y PET/CT.

ROC curves analysis for resin and glass sphere radioembolizations together (Fig. 1b) showed the best threshold of 40 Gy using D_{66} (Se = 91%, Sp = 78%, PPV = 94%, NPV = 70% and AUC = 0.93 ± 0.05). Examples of CDVH demonstrating radiological response or progression are seen in Fig. 3.

Survival analysis

Table 2 summarizes median OS and PFS for glass and resin microspheres treatments. Kaplan–Meier curves of OS and PFS (Fig. 4) show a clear discrimination between groups as defined by the absorbed dose thresholds for glass and resin microspheres. Using the same cutoff of 40 Gy for either type of microspheres, similar discrimination was found with D_{66} (Fig. 5). Accordingly, D_{66}<40 Gy was used for the univariate and multivariate analyses.

As shown in Table 3, univariate analysis of OS demonstrated that Equ. glass TD <118 Gy, D_{66}<40 Gy and portal thrombosis correlated with worse prognosis using the Cox regression. Only Equ. glass TD <118 Gy and D_{66}<40 Gy correlated with worse PFS using univariate analysis.

Only Equ. glass TD <118 Gy and portal thrombosis statistically were associated with a worse OS in the multivariate analysis.

Discussion

The three main findings of this study can be summarized as follows. First, a relationship between ^{90}Y-PET-based tumor absorbed doses and patient outcome is established. Second, the difference in efficiency per absorbed dose between glass- and resin-microspheres is confirmed. Third, the DVH analysis, using $D_{66,}$ clearly highlights

Fig. 5

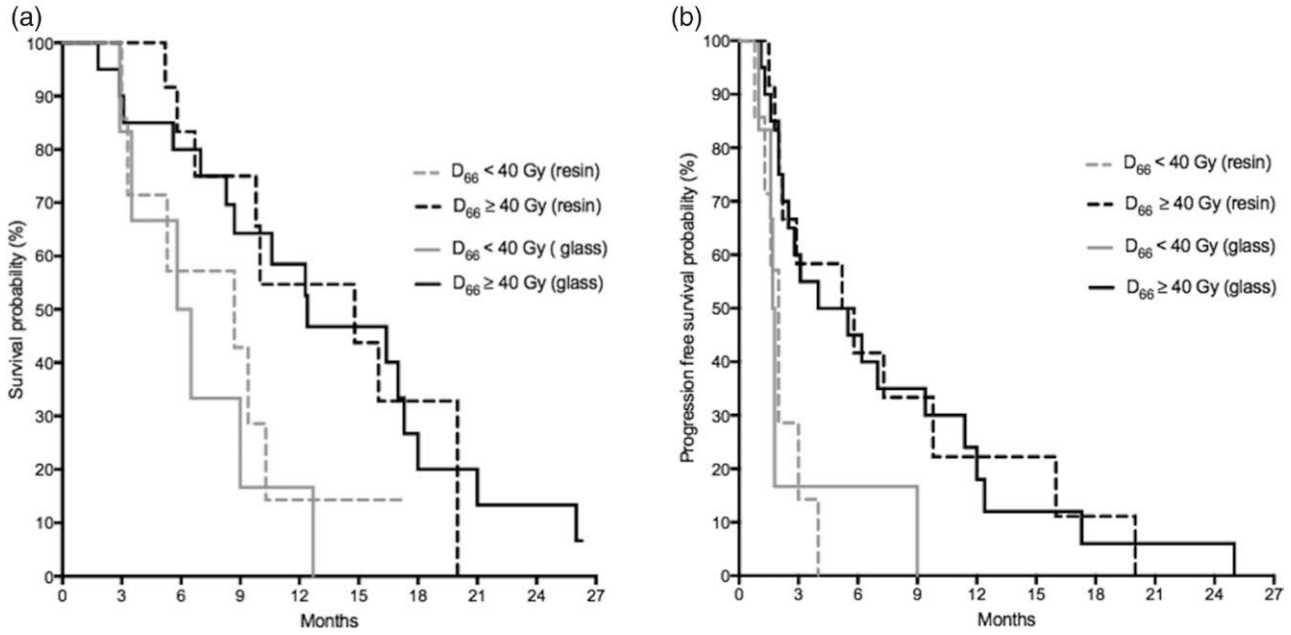

OS (a) and PFS (b) analyses with the Kaplan–Meier method using D_{66} with a threshold of 40 Gy for patients treated with glass and resin microspheres. OS, overall survival; PFS, progression-free survival.

Table 3 Overall survival and progression-free survival Cox analyses

		Univariate analysis		Multivariate analysis	
	Factors	HR (95% CI)	*P* value	HR (95% CI)	*P* value
OS	Equ. glass $TD^+ < 118$ Gy	5.9 (2.6–13.7)	<0.001	17.9 (3.2–100)	<0.001
	$D_{66} < 40$ Gy	2.9 (1.4–6.1)	0.006	0.3 (0.1–1.7)	0.18
	Portal thrombosis	2.9 (1.3–6.4)	0.07	3.5 (1.4–9.1)	0.01
PFS	TD < 118 Gy	3.3 (1.6–6.8)	0.001	1.8 (0.6–5.5)	0.28
	$D_{66} < 40$ Gy	3.4 (1.7–7)	0.001	2.3 (0.7–7.0)	0.15

CI, confidence interval; HR, hazard ratio; Equ. glass TD^+: equivalent glass microsphere tumor absorbed mean dose.

that the heterogeneity of tumor deposition is an essential parameter of clinical outcome.

Based on ROC curves analysis (Fig. 2a), the best-absorbed dose cutoffs for responses according to mRECIST criteria were 61 and 118 Gy for resin and glass microspheres, respectively. This represents a 1.9 ratio between the glass and resin microspheres. By multiplying the absorbed dose of each individual tumor treated with resin microspheres by this 1.9 factor while keeping the absorbed dose value for the glass sphere, we generated an effective dose, which was further input in the uni- and multivariate analyses. This 118 Gy, effective dose cutoff, applied to patients treated with either device, results in the best prediction factor in the multivariate analysis for OS, but not for PFS. This 1.9 factor is in agreement with previous data regarding toxicity, efficiency and clinical outcome.

The 118 Gy-threshold for glass radioembolization is remarkably lower than MAA-SPECT-based 205 Gy-threshold found by Garin *et al.* [21]. Besides the numerous differences in the absorbed doses' assessment, a careful analysis of this study shows that this 205 Gy value was especially highly discriminating in patients with portal vein thrombosis (2–8 months survival for TD <205 Gy vs. 9.5–27 months survival for TD >205 Gy). For the overall patient population, the large overlap in survival (3–24 months for TD<205 Gy vs. 15–27 months for TD >205 Gy) indicates that this threshold value is likely too high.

For liver toxicity, the tolerable whole liver absorbed dose has been reported to be 40 Gy with resin and 70 Gy for glass microspheres (factor: 1.8) [5]. Monte-Carlo simulations of the microspheres transport from the catheter tip provide a theoretical explanation of this feature [22] nicely confirmed in an animal model [23]. Moreover, the mean tumor absorbed dose is ~two-fold higher for glass microspheres than for resin microspheres to get similar EUD [17].

It is well known that absorbed doses needed for efficient radioembolization are higher than those needed with external beam radiotherapy, either conventional or stereotactic. The main cause is the heterogeneous dose distribution, depending on the arterial tumor microvasculature for radioembolization. Analysis of ^{90}Y-TOF-PET-based CDVH can explain why some tumors progress despite high absorbed dose (heterogeneous distribution) and why some tumors respond despite lower absorbed doses (homogeneous distribution) (Fig. 3). Owing to its excellent spatial resolution, ^{90}Y-TOF-PET has the ability to assess the tumor dose deposition at the voxel level [17–19]. Monte Carlo simulations of microspheres in the hepatic arterial tree also confirmed a good matching between the spheres distribution texture and ^{90}Y-TOF-PET imaging [24,25].

In our study, the prediction was improved, regarding OS and PFS, using a D_{66} cutoff of 40 Gy for both types of microspheres (Fig. 5). This D_{66} cutoff reconciles dose levels between external beam radiotherapy (EBRT) and radioembolization [26]. D_{70} has already been used in order to predict patient outcome. In a series of eight patients, Kao *et al.* [15] reported a D_{70} threshold of 100 Gy in order to obtain a complete response. However, in line with our study, Flower *et al.* [16] reported an optimal D_{70} threshold of 42 Gy for predicting response in 24 patients treated by resin or glass microspheres.

It could appear weird that observing only 66% of the tumor volume above 40 Gy is the best cutoff to differentiate worse and improved patient outcome while it is commonly observed in EBRT that 100% of the tumor volume has to be above 40 Gy in order to get a good response. Three reasons could explain this apparent discrepancy. First, the tumor VOI used to compute the based voxel dose can include small necrotic regions not tapping microspheres, which does not impact the outcome. Second, measured voxel dose at the boundary of the tumor is artificially reduced as a result of the limited spatial resolution of human PET imaging. Last, inside the tumor, some measured voxel doses can also be artificially reduced by statistical fluctuations inherent to the acquisition of nuclear decays. All those effects together could explain, in the patient group with more favorable outcome, that although 34% of the tumor volume appears to have received less than the 40 Gy threshold with PET imaging, in reality, almost all the viable tumor volume received at least 40 Gy. This assumption could be evaluated by high-resolution PET/CT imaging of excised radioembolized tumors in an animal model.

Recent randomized controlled trials failed to demonstrate the superiority of radioembolization compared to sorafenib in advanced hepatocellular carcinoma [27,28]. No significant differences in OS and PFS were demonstrated in radioembolization and sorafenib arms. However, radioembolization was significantly better tolerated compared to sorafenib with a reduction of the frequency and the severity of side effects [29]. Regarding the dosimetric methodology of these trials, the planned activity was based on an empirical method, the body surface area, without any goal in tumor absorbed dose targeting. This activity planification is known to be responsible for underdosing tumors in many cases [30]. A recent secondary analysis of the SARAH trial demonstrated that a higher tumor absorbed dose, using MAA SPECT-CT, was associated with better OS in HCC [31]. Also, as previously demonstrated with dosimetry based on MAA-Tc^{99m} imaging [21,31], ^{90}Y SPECT [10] or recent data using ^{90}Y-PET [32], we found a strong relationship between measured tumor absorbed doses and clinical response. In future prospective trials, tumor absorbed dose evaluation should clearly be taken into account to anticipate better outcomes as compared to other therapies available in HCC.

Study limitations

This study suffers from some limitations related to its retrospective nature. First, the choice of the device was not randomized and was clinically driven. Glass microspheres were mostly used in more aggressive HCC lesions (with vascular invasion). Second, patients were allowed later on to any therapy following radioembolization, which happened to more than 1/3 of the patients. It should be noted, however, that similar therapies were offered after glass and resin microspheres.

Conclusion

These results demonstrate the importance of tumor dose analysis after radioembolization in HCC using ^{90}Y-PET. A systematic evaluation of dose parameters could predict radiological response and patient outcome directly after treatment. In case of low estimated absorbed doses, patient management could be reevaluated and adapted quickly even before radiological response assessment.

Acknowledgments

We are grateful to Lieven Desmet from the Statistical Methodology and Computing Unit of UCL for advice and help in the statistical analysis.

Philippe d'Abadie is supported by the 'Fonds de Recherche Clinique' of the Cliniques universitaires St-Luc, Brussels.

Conflicts of interest

There are no conflicts of interest.

References

1 Kallini JR, Gabr A, Salem R, Lewandowski RJ. Transarterial radioembolization with yttrium-90 for the treatment of hepatocellular carcinoma. *Adv Ther* 2016; **33**:699–714.

2 Salem R, Gabr A, Riaz A, Mora R, Ali R, Abecassis M, *et al.* Institutional decision to adopt Y90 as primary treatment for hepatocellular carcinoma informed by a 1,000-patient 15-year experience. *Hepatology* 2018; **68**:1429–1440.

3 Van Der Gucht A, Jreige M, Denys A, Blanc-Durand P, Boubaker A, Pomoni A, *et al*. Resin versus glass microspheres for 90Y transarterial radioembolization: comparing survival in unresectable hepatocellular carcinoma using pretreatment partition model dosimetry. *J Nucl Med* 2017; **58**:1334–1340.
4 Giammarile F, Bodei L, Chiesa C, Flux G, Forrer F, Kraeber-Bodere F, *et al*.; Therapy, Oncology and Dosimetry Committees. EANM procedure guideline for the treatment of liver cancer and liver metastases with intra-arterial radioactive compounds. *Eur J Nucl Med Mol Imaging* 2011; **38**:1393–1406.
5 Cremonesi M, Chiesa C, Strigari L, Ferrari M, Botta F, Guerriero F, *et al*. Radioembolization of hepatic lesions from a radiobiology and dosimetric perspective. *Front Oncol* 2014; **4**:210.
6 Flamen P, Vanderlinden B, Delatte P, Ghanem G, Ameye L, Van Den Eynde M, Hendlisz A. Multimodality imaging can predict the metabolic response of unresectable colorectal liver metastases to radioembolization therapy with yttrium-90 labeled resin microspheres. *Phys Med Biol* 2008; **53**:6591–6603.
7 Garin E, Lenoir L, Rolland Y, Edeline J, Mesbah H, Laffont S, *et al*. Dosimetry based on 99mTc-macroaggregated albumin SPECT/CT accurately predicts tumor response and survival in hepatocellular carcinoma patients treated with 90Y-loaded glass microspheres: preliminary results. *J Nucl Med* 2012; **53**:255–263.
8 Chiesa C, Maccauro M, Romito R, Spreafico C, Pellizzari S, Negri A, *et al*. Need, feasibility and convenience of dosimetric treatment planning in liver selective internal radiation therapy with (90)Y microspheres: the experience of the National Tumor Institute of Milan. *Q J Nucl Med Mol Imaging* 2011; **55**:168–197.
9 Strigari L, Sciuto R, Rea S, Carpanese L, Pizzi G, Soriani A, *et al*. Efficacy and toxicity related to treatment of hepatocellular carcinoma with 90Y-SIR spheres: radiobiologic considerations. *J Nucl Med* 2010; **51**:1377–1385.
10 Kappadath SC, Mikell J, Balagopal A, Baladandayuthapani V, Kaseb A, Mahvash A. Hepatocellular carcinoma tumor dose response after 90Y-radioembolization with glass microspheres using 90Y-SPECT/CT-based voxel dosimetry. *Int J Radiat Oncol Biol Phys* 2018; **102**:451–461.
11 Lhommel R, Goffette P, Van den Eynde M, Jamar F, Pauwels S, Bilbao JI, Walrand S. Yttrium-90 TOF PET scan demonstrates high-resolution biodistribution after liver SIRT. *Eur J Nucl Med Mol Imaging* 2009; **36**:1696.
12 Lhommel R, van Elmbt L, Goffette P, Van den Eynde M, Jamar F, Pauwels S, Walrand S. Feasibility of 90Y TOF PET-based dosimetry in liver metastasis therapy using SIR-spheres. *Eur J Nucl Med Mol Imaging* 2010; **37**:1654–1662.
13 Walrand S, Lhommel R, Goffette P, Van den Eynde M, Pauwels S, Jamar F. Hemoglobin level significantly impacts the tumor cell survival fraction in humans after internal radiotherapy. *EJNMMI Res* 2012; **2**:20.
14 Kennedy AS, Ball D, Cohen SJ, Cohn M, Coldwell DM, Drooz A, *et al*. Baseline hemoglobin and liver function predict tolerability and overall survival of patients receiving radioembolization for chemotherapy-refractory metastatic colorectal cancer. *J Gastrointest Oncol* 2017; **8**:70–80.
15 Kao YH, Steinberg JD, Tay YS, Lim GK, Yan J, Townsend DW, *et al*. Post-radioembolization yttrium-90 PET/CT - part 2: dose-response and tumor predictive dosimetry for resin microspheres. *EJNMMI Res* 2013; **3**:57.
16 Fowler KJ, Maughan NM, Laforest R, Saad NE, Sharma A, Olsen J, *et al*. PET/MRI of hepatic 90Y microsphere deposition determines individual tumor response. *Cardiovasc Intervent Radiol* 2016; **39**:855–864.
17 d'Abadie P, Hesse M, Jamar F, Lhommel R, Walrand S. 90Y TOF-PET based EUD reunifies patient survival prediction in resin and glass microspheres radioembolization of HCC tumours. *Phys Med Biol* 2018; **63**:245010.
18 Walrand S, Hesse M. PET/CT specificities in 90Y imaging post radioembolization. *PET Clin* 2019; **14**:469–476.
19 Walrand S, Hesse M. Significant artefactual noise in 90Y TOF-PET imaging of low specific activity phantoms arises despite increased acquisition time. *EJNMMI Phys* 2019; **6**:20.
20 Padia SA, Lewandowski RJ, Johnson GE, Sze DY, Ward TJ, Gaba RC, *et al*.; Society of Interventional Radiology Standards of Practice Committee. Radioembolization of hepatic malignancies: background, quality improvement guidelines, and future directions. *J Vasc Interv Radiol* 2017; **28**:1–15.
21 Garin E, Rolland Y, Pracht M, Le Sourd S, Laffont S, Mesbah H, *et al*. High impact of macroaggregated albumin-based tumour dose on response and overall survival in hepatocellular carcinoma patients treated with 90 Y-loaded glass microsphere radioembolization. *Liver Int* 2017; **37**:101–110.
22 Walrand S, Hesse M, Jamar F, Lhommel R. A hepatic dose-toxicity model opening the way toward individualized radioembolization planning. *J Nucl Med* 2014; **55**:1317–1322.
23 Pasciak AS, Abiola G, Liddell RP, Crookston N, Besharati S, Donahue D, *et al*. The number of microspheres in Y90 radioembolization directly affects normal tissue radiation exposure. *Eur J Nucl Med Mol Imaging* 2020; **47**:816–827.
24 Walrand S, Hesse M, Chiesa C, Lhommel R, Jamar F. The low hepatic toxicity per Gray of 90Y glass microspheres is linked to their transport in the arterial tree favoring a nonuniform trapping as observed in posttherapy PET imaging. *J Nucl Med* 2014; **55**:135–140.
25 Crookston NR, Fung G, Frey E. Development of a customizable hepatic arterial tree and particle transport model for use in treatment planning. *IEEE Trans Radiat Plasma Med Sci* 2019; **3**:31–37.
26 Sanuki N, Takeda A, Kunieda E. Role of stereotactic body radiation therapy for hepatocellular carcinoma. *World J Gastroenterol* 2014; **20**:3100–3111.
27 Vilgrain V, Pereira H, Assenat E, Guiu B, Ilonca AD, Pageaux GP, *et al*.; SARAH Trial Group. Efficacy and safety of selective internal radiotherapy with yttrium-90 resin microspheres compared with sorafenib in locally advanced and inoperable hepatocellular carcinoma (SARAH): an open-label randomised controlled phase 3 trial. *Lancet Oncol* 2017; **18**:1624–1636.
28 Chow PKH, Gandhi M, Tan SB, Khin MW, Khasbazar A, Ong J, *et al*.; Asia-Pacific Hepatocellular Carcinoma Trials Group. SIRveNIB: selective internal radiation therapy versus sorafenib in Asia-Pacific patients with hepatocellular carcinoma. *J Clin Oncol* 2018; **36**:1913–1921.
29 Sposito C, Mazzaferro V. The SIRveNIB and SARAH trials, radioembolization vs. sorafenib in advanced HCC patients: reasons for a failure, and perspectives for the future. *Hepatobiliary Surg Nutr* 2018; **7**:487–489.
30 Bastiaannet R, Kappadath SC, Kunnen B, Braat AJAT, Lam MGEH, de Jong HWAM. The physics of radioembolization. *EJNMMI Phys* 2018; **5**:22.
31 Hermann AL, Dieudonné A, Ronot M, Sanchez M, Pereira H, Chatellier G, *et al*.; SARAH Trial Group. Relationship of tumor radiation-absorbed dose to survival and response in hepatocellular carcinoma treated with transarterial radioembolization with 90Y in the SARAH study. *Radiology* 2020; **296**:673–684.
32 Dewaraja YK, Devasia T, Kaza RK, Mikell JK, Owen D, Roberson PL, Schipper MJ. Prediction of tumor control in 90Y radioembolization by logit models with PET/CT-based dose metrics. *J Nucl Med* 2020; **61**:104–111.